

## Computer analysis of the axial-to-planar channeling transition: Linkage with continuum theory

A. Desalvo\* and R. Rosa

*Laboratorio di Chimica e Tecnologia dei Materiali e Componenti per l'Elettronica, Consiglio Nazionale delle Ricerche, 40126, Bologna, Italy*

(Received 3 August 1973)

A systematic computer analysis of the transition between channeling along the  $\langle 110 \rangle$  axis and along the most important planes intersecting it ( $\{111\}$ ,  $\{110\}$ , and  $\{100\}$ ) of 1-MeV protons in silicon is carried out. It is shown that, as the tilt angle varies, the transition between the two channeling regimes does not take place gradually, but occurs by passing through an angular region in which dechanneling is maximum. An analysis of the ion trajectories in a four-dimensional reduced phase space shows that in this transition region the occupied volume is maximum, which explains the experimental effects observed by different authors. The transition is also clearly displayed when the incidence angle is tilted from the axis within the most open plane, which shows that axial and planar channeling cannot simply be reduced one to the other. An interpretation in terms of Lindhard's continuum theory is worked out, giving results in satisfactory agreement with computer simulations.

### I. INTRODUCTION

In a previous paper<sup>1</sup> it was shown that the stopping power does not vary steadily but gives rise to a maximum as the incidence angle with a crystallographic axis is increased while keeping the incidence direction in a crystallographic plane. We recall that this shoulder remains lower than the random value; moreover corresponding to the maximum in the stopping power there is also a maximum in the dechanneled fraction of the beam. The phenomenon was also reproduced by computer simulations.

Similar effects have been observed experimentally in  $(p, \gamma)$  nuclear reactions,<sup>2</sup> transmitted intensity of protons (the so called star patterns),<sup>3</sup> nuclear backscattering,<sup>4,5</sup> and theoretically by computer simulation of the nuclear-encounter probability.<sup>6</sup> However, specific attention to this effect is found only in the papers by Dearnaley and co-workers.<sup>3</sup>

In this paper we systematically analyze the axial-to-planar channeling transition by computer and try to interpret it in terms of the familiar Lindhard's continuum theory.<sup>7</sup> The practical usefulness of the latter theory compared to a Monte Carlo simulation is beyond dispute as far as the computer time is concerned. An investigation of the correspondence among the results of the Monte Carlo computer simulations, which are more detailed but require a longer elaboration, and the simpler analytical expressions of the continuum theory can afford a more extensive application of the latter.

The analysis is carried out for the most important planes intersecting the same axis; as is well known, sometimes axial channeling has been regarded simply as a superposition of planar channeling through these planes.<sup>8</sup> Particular attention

was paid to display the transition in the case of the most open plane intersecting the axis; in fact axial channeling actually corresponds to an erratic motion through neighboring channels, which, at first sight, would seem to support the previously mentioned point of view.

### II. COMPUTER MODEL

The computer model was already described in detail in a series of other papers<sup>1,9</sup>; we recall here only the main features for the reader's convenience: (a) The interaction between the incident ion and the crystal atoms is evaluated according to the classical momentum approximation; the potential employed is the standard Lindhard's potential. (b) Proper allowance for impact-parameter dependence of the stopping power is made by using Eq. (3.15) of Ref. 7, without assuming equipartition between close and distant collisions and simply taking  $\alpha$  as an experimental parameter which varies with energy. (c) Thermal vibrations of the atoms of the crystal lattice and angular dispersion owing to electron scattering are accounted for in the usual way. (d) The position of the ion when it leaves the channel is "reduced" to the original channel each time by means of a suitable translation.

We analyzed the axial-to-planar channeling transition in detail, starting from the  $\langle 110 \rangle$  axis and moving along the  $\{111\}$ ,  $\{110\}$ , and  $\{100\}$  planes intersecting it, to see how the transition depends on interplanar distance.

The proton energy was 1.0 MeV. The starting point was always chosen to be the same, i.e., coincident with the center of the  $\langle 110 \rangle$  axial channel in the case of the  $\{111\}$  and  $\{100\}$  planes and shifted along the horizontal line (see below, Fig. 4) in order to coincide also with midplane position

for the  $\{110\}$  plane. This was done in order to reduce scatter in the results owing to differences in initial position. Moreover, our particular choice at the center of planes is such as to minimize dechanneling due to other effects (thermal vibrations and electron scattering) and therefore to display mostly the dechanneling effect due solely to the transition between the axial and planar regimes. Computations were carried out with the CDC 6600 of the "Centro di Calcolo Elettronico Interuniversitario dell'Italia Nord-Orientale" of Bologna.

### III. RESULTS

Figure 1 shows the average penetration under axial- and planar-channeling conditions as the incidence angle with the  $\langle 110 \rangle$  axis increases for the different transitions. We recall that, while planar channeling ends when the ion leaves the planar channel, in axial channeling the ion wanders from channel to channel. Therefore we assumed the same statistical criterion as in our previous paper, which compares the number of collisions with a string closer than a certain distance of approach (taken equal to the Thomas-Fermi screening radius) with the corresponding number occurring in a random ion path.<sup>1</sup> The points are averages taken over a certain number of computed paths ( $\sim 10$ ) which differ in the sequence of the random numbers used to simulate thermal vibrations and electron scattering. For very small incidence angles (axial channeling) the paths become very long and are no longer shown in the figure.

Figure 1 shows clearly the following points: (i) There is an angular region for which dechanneling is maximum, i. e., the channeled path is minimum. (ii) At lower angles the ion covers only a short distance along the planar channel and then

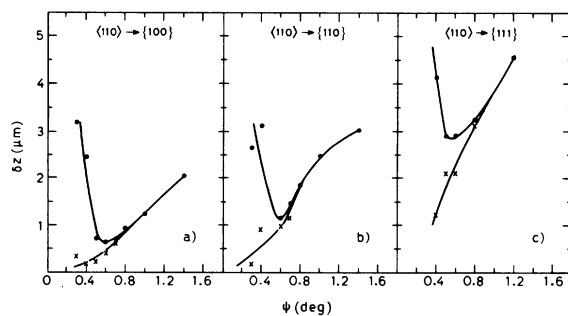


FIG. 1. Penetration depth  $\delta z$  of channeled 1-MeV protons in silicon versus incidence angle  $\psi$  with  $\langle 110 \rangle$  axis, tilting along different planes:  $\times$ , penetration depth under planar-channeling conditions;  $\bullet$ , penetration depth under axial-channeling conditions.

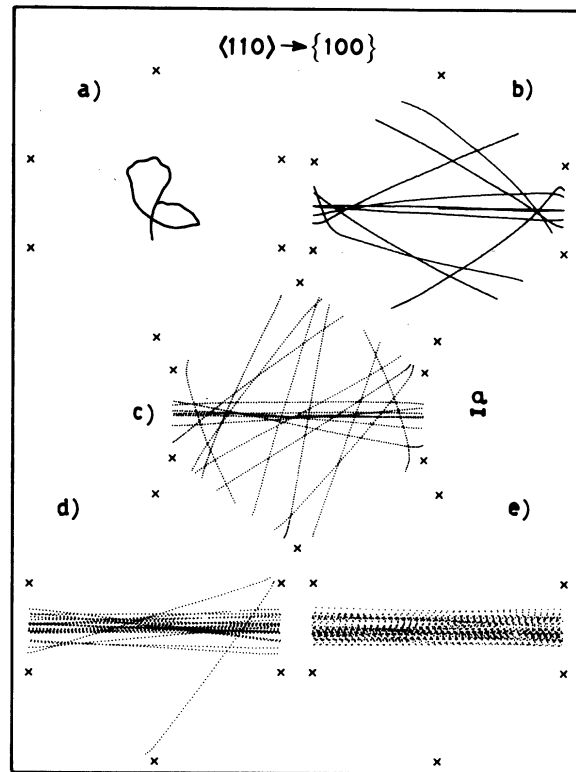


FIG. 2. Computed paths of 1-MeV protons in a  $0.6\text{-}\mu\text{m}$  silicon crystal, for different tilting angles  $\psi$  from the  $\langle 110 \rangle$  axis, within the  $\{100\}$  plane, and reduced in the initial channel. The starting point is always at midchannel axis. The Thomas-Fermi screening radius  $a$  is shown for comparison: (a)  $\psi = 0^\circ$ ; (b)  $\psi = 0.4^\circ$ ; (c)  $\psi = 0.6^\circ$ ; (d)  $\psi = 0.8^\circ$ ; (e)  $\psi = 1.4^\circ$ .

travels under axial channeling conditions, the penetration depth increasing with decreasing incidence angle. (iii) At higher angles, when the ion leaves the planar channel, it moves directly along a random path; the penetration depth along a planar channel increases as the incidence angle with the  $\langle 110 \rangle$  axis increases, approaching more and more a purely-planar-channeling behavior. (iv) The angle at which the transition occurs does not seem to depend critically on the type of plane. It must be pointed out that the transition angle we find here cannot be compared directly with the one found in our previous work, because in the latter case an average among all the different starting positions of the incident ion is involved. On the contrary the figure clearly shows that the channeled path in the transition region decreases strongly with decreasing interplanar distance.

Figures 2-7 show a more detailed analysis of the trajectories, both in two-dimensional coordinate space (even though "reduced" in the initial

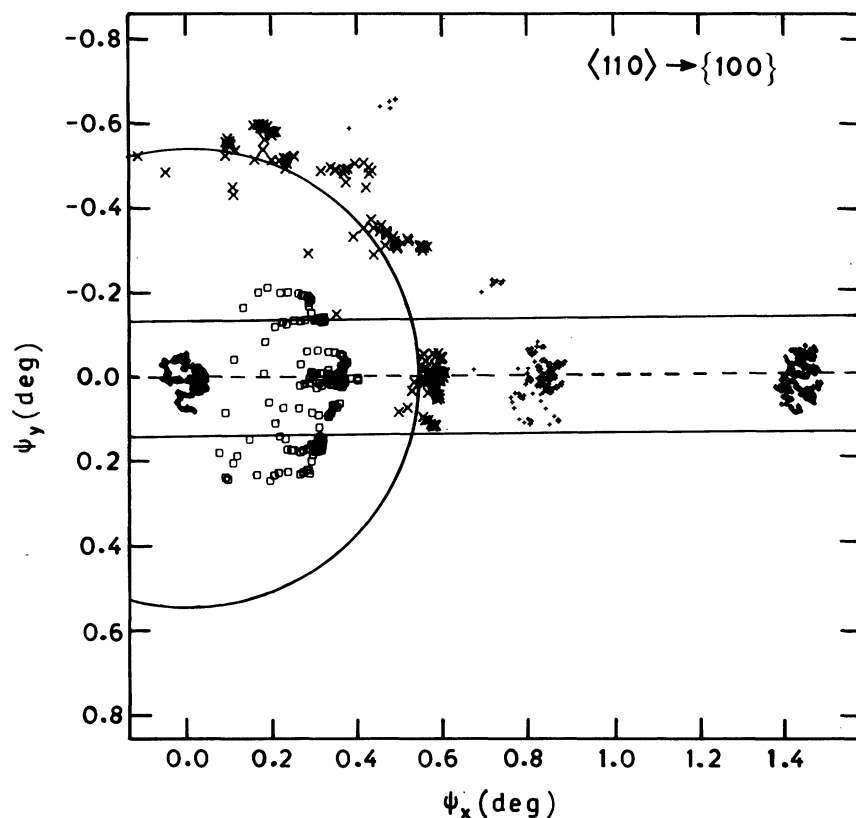


FIG. 3. Computed transverse angles corresponding to the paths shown in Fig. 2. The dashed line is the trace of the  $\{100\}$  plane. The continuous lines and circle give the critical angle for planar and axial channeling respectively.  $\bullet$ ,  $\psi = 0^\circ$ ;  $\square$ ,  $\psi = 0.4^\circ$ ;  $\times$ ,  $\psi = 0.6^\circ$ ;  $+$ ,  $\psi = 0.8^\circ$ ;  $\circ$ ,  $\psi = 1.4^\circ$ .

channel) and in two-dimensional momentum space (actually the figures show the scattering angles, which are proportional to transverse-momentum components, neglecting the energy loss, as is legitimate for small thicknesses at these energies). The coordinates  $x$  and  $y$  used in Figs. 3, 5, and 7 correspond to the momentum components along the horizontal and vertical directions of Figs. 2, 4, and 6. The penetration depth of the ion is taken to be the same for every transition and equal to the value of the minimum penetration of Fig. 1 (i. e.,  $0.6 \mu\text{m}$  for the  $\langle 110 \rangle - \{100\}$  transition,  $1.1 \mu\text{m}$  for the  $\langle 110 \rangle - \{110\}$  transition, and  $2.9 \mu\text{m}$  for the  $\langle 110 \rangle - \{111\}$  transition).

Figures 2 and 3 show the behavior in the phase space for the  $\langle 110 \rangle - \{100\}$  transition. The typical points chosen give the following sequence. At  $0^\circ$  the channeling is purely axial and the particle remains confined in a very limited zone of the four-dimensional reduced phase space. At  $0.4^\circ$  the "memory" of planar channeling is very limited; the particle tends to fill rapidly, in a relatively isotropic way, both coordinate and momentum space, keeping, however, at larger distances than  $a$  from the strings and inside the critical angle  $\psi_c$ . At  $0.6^\circ$  the planar-channeled path becomes much more easily recognizable in both spaces, but the particle acquires a component

perpendicular to the plane, which leads it to hit the atomic rows and increases the angle beyond the critical one. At  $0.8^\circ$  the planar-dechanneling event occurs only at the end of the path and is immediately followed by axial dechanneling. Finally at  $1.4^\circ$  we are in a purely planar regime.

Figures 4 and 5 show the same thing for the  $\langle 110 \rangle - \{110\}$  transition. We notice that when planar channeling occurs in coordinate space two strips appear, which are obviously due to the coordinate translation undergone by the particle any time it crosses the axial-channel boundary. The general trend is very similar to the one shown in Figs. 2 and 3. The only visible differences are that at  $0.4^\circ$  the point distribution in phase space is less isotropic than in the previous case and that at  $0.8^\circ$  the final dechanneling event has not yet occurred. But it must be noticed that these fluctuations in behavior among different points corresponding to the same incidence angle appear in each of the analyzed transitions and therefore do not seem to depend upon the particular nature of the crystal plane.

Finally, Figs. 6 and 7 refer to  $\langle 110 \rangle - \{111\}$  transition, i. e., to the most open intersecting plane. The first point to emphasize is that a transition also occurs distinctly in this rather unexpected case. Figure 6(a) shows clearly that

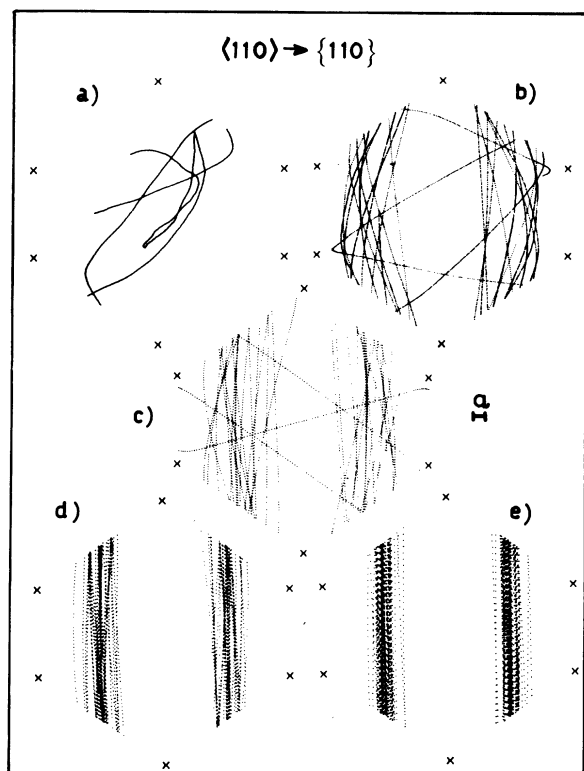


FIG. 4. Same as Fig. 2, except that the crystal thickness is  $1.1 \mu\text{m}$  and the tilting is along the  $\{110\}$  plane. The starting point is clearly shown in Fig. 4(a) at the center of the  $\{110\}$  plane, displaced to the left of the center of the axial channel along a horizontal line: (a)  $\psi = 0^\circ$ ; (b)  $\psi = 0.4^\circ$ ; (c)  $\psi = 0.6^\circ$ ; (d)  $\psi = 0.8^\circ$ ; (e)  $\psi = 1.4^\circ$ .

at zero incidence the particle goes through the saddle points in a direction almost parallel to the  $\{111\}$  plane, along which the potential gradient is minimum. However, Figs. 6(b)–6(e) show clearly that this random motion through the saddle points is not equivalent to a simple superposition of planar paths! Also, in this case the general trend is similar to the ones previously shown. At  $0.4^\circ$  and  $0.6^\circ$  a higher isotropy is observed, which is almost certainly due to the larger thickness traveled by the ion. We notice that Fig. 6(d) is much more similar to Fig. 2(d) than to Fig. 4(d) and that the purely planar case corresponds to an incidence angle with the  $\langle 110 \rangle$  axis equal to  $1.2^\circ$  instead of  $1.4^\circ$  as in the previous figures.

In conclusion, the figures show clearly that in the transition region the extension of the trajectory is maximum both in direct and momentum space. This accounts for the previously mentioned experimental results (maximum value of nuclear reaction<sup>2</sup> and Rutherford backscattering<sup>4,5</sup> yields and of stopping power<sup>1</sup>). For smaller and larger

angles a progressive shrinking of the region occupied in phase space occurs, finally giving rise to the phase-space distribution expected for axial and planar channeling, respectively. If we start from purely-planar-channeling conditions we see that as the incidence angle with the atomic row decreases, a transverse-energy component normal to the plane appears, which increases rapidly and produces the penetration of the particle in the plane and its consequent dechanneling. However, when the angle with the atomic string becomes small enough, the effect of the single string prevails, i. e., in the language of the continuum theory "the string stands out distinctly within a plane."<sup>7</sup> In other words, the acquired transverse energy is sufficient to penetrate into the plane, imagined as a string of strings, but not into the single string. At still lower angles the ion interacts therefore with a single string for once, without "seeing" the crystallographic planes any more.

#### IV. DISCUSSION

According to the latter statements, we tried to interpret quantitatively our results in terms of continuum theory. A few words must be said about the limitations of this attempt. In fact, it is obvious that we cannot obtain a quantitative agreement for at least two fundamental reasons: The first one is that we ought to have a very large number of computer-simulated trajectories in order to pass to the limit of continuum theory. The second reason is more fundamental; in fact, it is difficult to employ the concepts of continuum theory just at their limits of validity, i. e., when the plane ceases to appear continuous to the incident ion. However, what seemed of particular interest was that the continuum theory also contains the possibility of treating this case, at least in first approximation.

Let us consider the analysis of the limits of validity of continuum theory for a string of atoms (see Appendix A of Ref. 7) and apply it to a plane treated as a string of strings. In the following we shall denote with  $\psi$  the angle with the atomic string (we recall that in our case the incidence direction lies in the lattice plane) and with  $\varphi_1$  the angle with the lattice plane projected in the transverse plane normal to the atomic row. As a consequence the angle of the ion path with the lattice plane is given by  $\psi_1 = \varphi_1 \psi$  (see p. 19 of Ref. 7). Unless otherwise specified, the symbols have the same meaning as in Ref. 7. In this notation Eq. (A.12) of Ref. 7 becomes

$$(\delta E_1)_d = \delta(E\varphi_1^2\psi^2) = d_s^2 Y'(r_{\text{min}})/48E\psi^2, \quad (1)$$

where  $(\delta E_1)_d$  is evaluated over all impact parameters. This dechanneling mechanism must be added to the other ones usually taken into account,

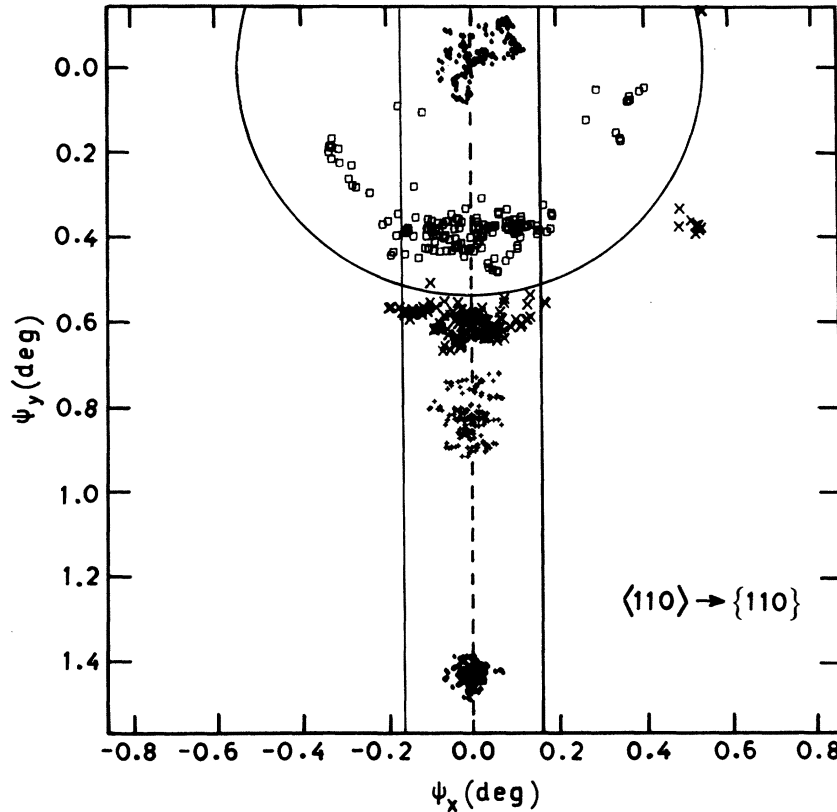


FIG. 5. Computed transverse angles corresponding to the paths shown in Fig. 4. The dashed line is the trace of the  $\{110\}$  plane. Continuous lines and circle have the same meaning as in Fig. 3:  $\bullet$ ,  $\psi = 0^\circ$ ;  $\square$ ,  $\psi = 0.4^\circ$ ;  $+$ ,  $\psi = 0.8^\circ$ ;  $\bullet$ ,  $\psi = 1.4^\circ$ .

i. e., thermal vibrations and electron scattering. As is well known, the latter is the prevailing dechanneling mechanism in the planar case.<sup>4,10</sup>

In the following the various contributions are evaluated separately. If we use the planar Lindhard's potential, we obtain

$$d_s Y'(y) = \frac{2\pi Z_1 Z_2 e^2}{d} \times \left[ \left( 1 + \frac{C^2 a^2}{y^2} \right)^{-1/2} - \left( 1 + \frac{C^2 a^2}{(d_p - y)^2} \right)^{-1/2} \right]. \quad (2)$$

It is difficult to say what is the appropriate value of  $r_{\min}$  to be put in Eq. (1) because the effective path is oscillatory with increasing amplitude up to the final dechanneling. The choice made in the following is not unreasonable and gives results in good agreement, as order of magnitude, with the Monte Carlo results. The main drawback of Eq. (1) is that it does not give an explicit dependence of the transverse-energy variation on depth, which does not seem realistic. Of course, at very low values of  $E\psi^2$ ,  $(\delta E_1)_d$  becomes so high that dechanneling occurs for very low thicknesses and the use of Eq. (1), which implies that  $E_1$  is approximately conserved, becomes problematic. If we put  $r_{\min} = a$  (Thomas-Fermi screening radius),

the term between brackets becomes equal to about 0.5. For 1-MeV protons along  $\langle 110 \rangle$  axis in silicon ( $d = 3.84 \text{ \AA}$ ) and  $\psi = 0.6^\circ = 1.05 \times 10^{-2} \text{ rad}$  (transition region) we obtain  $(\delta E_1)_d \cong 5 \text{ eV}$ . This transverse-energy component decreases rapidly with increasing incidence angle  $\psi$  and becomes negligible compared to the normal dechanneling due to electron scattering.

The latter may be estimated as follows:

$$(\delta E_1)_e = \frac{m}{4M_1} \left( \frac{dE}{dx} \right)_c \delta z, \quad (3)$$

where  $\delta z$  is the crystal thickness and one of the  $\frac{1}{2}$  factors stems from the fact that only the angular component of electron scattering perpendicular to the plane is effective for dechanneling<sup>10</sup> and the other one stems from taking into account only close collisions with valence electrons.<sup>11,12</sup> Since we do not assume any equipartition rule in calculating the stopping power under channeling conditions (see footnote 17 of Ref. 1), our model does not give zero electron scattering at the center of the channel. By using the same values of our computer model, i. e.,  $(-dE/dx)_c = \frac{1}{2} (-dE/dx)_R$ ,<sup>1,13</sup> and  $(-dE/dx)_R = 3.8 \text{ eV/\AA}$  (evaluated according to Lindhard and Scharff's model<sup>14</sup>), one obtains

$$(\delta E_1)_e = 2.6 \delta z \quad (\text{in eV, } \delta z \text{ in } \mu\text{m}). \quad (3')$$

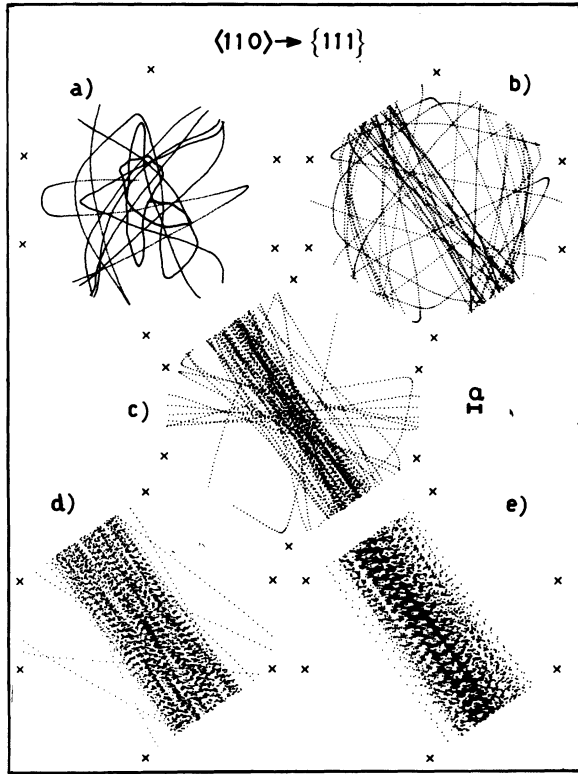


FIG. 6. Same as Figs. 2 and 4, except that the crystal thickness is  $2.9 \mu\text{m}$  and the tilting is along the  $\{111\}$  plane. The starting point is at midchannel axis, as in Fig. 2: (a)  $\psi = 0^\circ$ ; (b)  $\psi = 0.4^\circ$ ; (c)  $\psi = 0.6^\circ$ ; (d)  $\psi = 0.8^\circ$ ; (e)  $\psi = 1.2^\circ$ .

With increasing transverse energy this term increases (see, e.g., Ref. 10). However, we will limit ourselves to this simple expression because it is sufficient for our estimates.

First of all we may calculate the asymptotic values to which the curves of Fig. 1 tend with increasing incidence angles. If one puts  $(\delta E_{1e}) = E\psi_p^2$ , where<sup>15</sup>

$$\psi_p = 1.5(Z_1 Z_2 e^2 N d_p a / E)^{1/2}, \quad (4)$$

the results shown in the fourth column of Table I are obtained, in satisfactory agreement with the curves of Fig. 1.

The same procedure may be applied to the transition region [ $\psi = 0.6^\circ$ ,  $(\delta E_{1d}) = 5 \text{ eV}$ ] by equating

$$E\psi_p^2 = (\delta E_{1e}) + (\delta E_{1d}). \quad (5)$$

The results are shown in the last column of Table I and again agree with the data of Fig. 1. It is possible to see that, without including many adjustable parameters, the main differences among the various crystal planes are properly shown.

Finally we must analyze the part of the curve of Fig. 1 on the left of the transition region. Here the term due to the discrete structure of the plane is very large and the ion is rapidly dechanneled from the plane. As expected, the lower the planar barrier the lower the penetration depth becomes. It may be expected that the transverse energy relative to the string at the end of the planar path will be of the order of  $E\psi_p^2 + E\psi^2$ . However, the results of Figs. 3, 5, and 7 show that the perpendicular and parallel components of the transverse energy do not simply add vectorially but fluctuate around a value of the order of  $E\psi^2$ . For  $\psi = 0.4^\circ$ , a transverse energy of  $\sim 50 \text{ eV}$  is obtained. The contribution of thermal vibrations and electron scattering to dechanneling is now estimated in the axial case, using the expressions given by Lindhard<sup>7</sup>;

$$(\delta E_{1n}) = \frac{2\pi Z_1^2 Z_2^2 e^4}{E} N \frac{\rho^2}{C^2 a^2} e^{2E_1/E\psi_a^2} \times (1 - e^{-2E_1/E\psi_a^2})^3 \delta z, \quad (6)$$

where for  $\rho^2$  we use  $\frac{2}{3}$  of the mean quadratic amplitude of vibration.<sup>16</sup>

Taking into account that we use our Eq. (3) instead of Eq. (4.3) of Ref. 7, we obtain for electron scattering the following modification of Lindhard's expression:

$$(\delta E_{1e}) = \frac{m}{2M_1} \left( -\frac{dE}{dx} \right)_R (1 - \alpha e^{-2E_1/E\psi_a^2}) \delta z, \quad (7)$$

which does not go to zero at midchannel axis ( $E_1 = 0$ ) but gives a factor  $1 - \alpha = 0.5$ .

For  $\psi_a$  we used the expression corrected for temperature given by Barrett (see Ref. 17 for the meaning of symbols)

$$\psi_a = \kappa R(m\rho_x/a)\psi_1 = 0.54^\circ = 9.6 \times 10^{-3} \text{ rad}, \quad (8)$$

where  $\rho_x$  is  $\frac{1}{3}$  of the mean quadratic amplitude of vibration. With these values one obtains

$$(\delta E_{1n}) = 9.7 \delta z \text{ eV}, \quad (6')$$

$$(\delta E_{1e}) = 8.7 \delta z \text{ eV}. \quad (7')$$

Taking into account that dechanneling occurs when

$$E\psi_a^2 = E_1 + (\delta E_{1n}) + (\delta E_{1e}),$$

TABLE I. Penetration depth along the plane expected for 1-MeV protons in silicon in the purely planar regime,  $(\delta z)_p$ , evaluated according to Eq. (3'), and at the transition,  $(\delta z)_t$ , evaluated according to Eq. (5).

Plane	$\psi_p$ (rad)	$E\psi_p^2$ (eV)	$(\delta z)_p$ ( $\mu\text{m}$ )	$(\delta z)_t$ ( $\mu\text{m}$ )
{100}	$2.35 \times 10^{-3}$	5.5	2.1	0.2
{110}	$2.8 \times 10^{-3}$	7.8	3.0	1.1
{111}	$3.6 \times 10^{-3}$	13.0	5.0	3.0

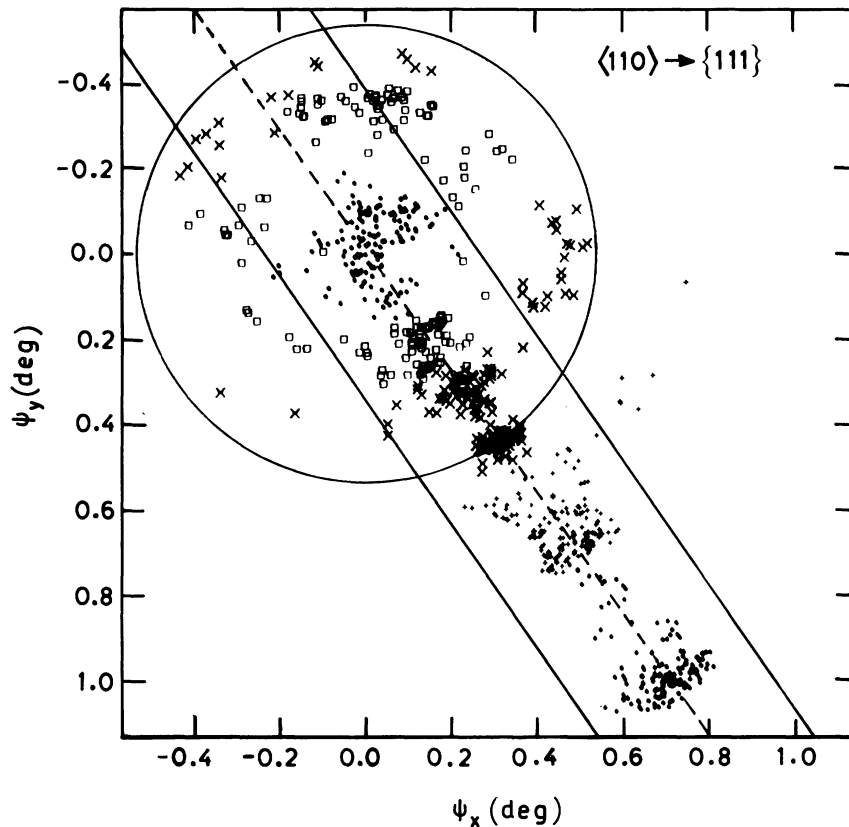


Fig. 7. Computed transverse angles corresponding to the paths shown in Fig. 6. The dashed line is the trace of the  $\{111\}$  plane. Continuous lines and circle have the same meaning as in Figs. 3 and 5.  $\bullet$ ,  $\psi = 0^\circ$ ;  $\square$ ,  $\psi = 0.4^\circ$ ;  $\times$ ,  $\psi = 0.6^\circ$ ;  $+$ ,  $\psi = 0.8^\circ$ ;  $\bullet$ ,  $\psi = 1.2^\circ$ .

one obtains  $\delta z = 2.2 \mu\text{m}$ , in satisfactory agreement with the data of Fig. 1, i. e.,  $2.8 \mu\text{m}$  for  $\{111\}$  plane and  $1.8 \mu\text{m}$  for  $\{110\}$  and  $\{100\}$  planes. At a still lower incidence angle the transverse energy relative to the string at the end of the planar-channeled path becomes much smaller (say of the order of  $E\psi^2$ ), and therefore we are in a purely axial regime.

#### V. CONCLUSIONS

This work shows, in a systematic and conclusive fashion, that the transition between axial and planar channeling does not occur in a gradual way but takes place through an angular region in which the channeled path is minimum. In the simple case we examined (protons starting from the center of the channel), the transition region does not depend very much on the nature of the plane and is placed around a value of the order of  $\psi_1$ , the Lindhard critical angle. The phenomenon may be explained by taking into account the discrete structure of the lattice plane, regarded as a string of strings. The nonconservation of transverse energy owing to this discrete structure can be evaluated according to Lindhard's theory and turns out to be of the right order of magnitude. This energy component is significant only at low transverse energies relative to the string:

Therefore with a decreasing incidence angle it becomes sufficient to penetrate the barrier for planar channeling. The conditions for a minimum channeled path are such that once the ion leaves the planar channel, the transverse energy relative to the strings is so high that it also immediately produces axial dechanneling. As  $E\psi^2$  still decreases, planar dechanneling occurs at once, but the transverse energy relative to the string is low and therefore purely axial channeling takes place.

We may therefore conclude that axial and planar channeling are qualitatively different. In other words, the angular region in which the motion of the ion is governed by single strings is clearly separated from the one in which the motion is governed by a string of strings. Perhaps this is not, after all, so surprising, if attention is paid to the fact that the former is fundamentally a two-dimensional problem and the latter one-dimensional, which makes a continuous transition between the two hard to imagine.

#### ACKNOWLEDGMENTS

It is a pleasure to express our sincere appreciation to G. G. Bentini, G. Della Mea, A. V. Drigo, S. Lo Russo, and P. Mazzoldi for the interesting problems opened by their experiments and for the fruitful discussions on the explanation of the same.

- \*Istituto Chimico, Facoltà di Ingegneria, Università di Bologna, Bologna, Italy.
- <sup>1</sup>G. Della Mea, A. V. Drigo, S. Lo Russo, P. Mazzoldi, G. G. Bentini, A. Desalvo, and R. Rosa, *Phys. Rev. B* **7**, 4029 (1973).
- <sup>2</sup>J. U. Andersen, J. A. Davies, K. O. Nielsen, and S. L. Andersen, *Nucl. Instrum. Methods* **38**, 210 (1965).
- <sup>3</sup>G. Dearnaley, B. W. Farmery, I. V. Mitchell, R. S. Nelson, and M. W. Thompson, in *Proceedings of the International Conference on Solid State Research with Accelerators*, Brookhaven, 1967, edited by A. N. Goland, BNL Report No. 50083, p. 125 (unpublished); G. Dearnaley, I. V. Mitchell, R. S. Nelson, B. W. Farmery, and M. W. Thompson, *Philos. Mag.* **18**, 985 (1968).
- <sup>4</sup>J. A. Davies, J. Denhartog, and J. L. Whitton, *Phys. Rev.* **165**, 345 (1968).
- <sup>5</sup>L. M. Howe and S. Schmid, *Can. J. Phys.* **49**, 2321 (1971).
- <sup>6</sup>J. H. Barrett, *Phys. Rev.* **166**, 219 (1968); T. S. Noggle and J. H. Barrett, *Phys. Status Solidi* **36**, 761 (1969).
- <sup>7</sup>J. Lindhard, *K. Dan. Vidensk. Selsk. Mat.-Fys. Medd.* **34**, No. 14 (1965).
- <sup>8</sup>B. R. Appleton, C. Erginsoy, H. E. Wegner, and W. M. Gibson, *Phys. Lett.* **19**, 185 (1965).
- <sup>9</sup>A. Desalvo, R. Rosa, and F. Zignani, *Nuovo Cimento Lett.* **2**, 390 (1971); *J. Appl. Phys.* **43**, 3755 (1972).
- <sup>10</sup>S. U. Campisano, G. Foti, F. Grasso, M. Lo Savio, and E. Rimini, *Rad. Effects* **13**, 157 (1972).
- <sup>11</sup>J. Lindhard, *K. Dan. Vidensk. Selsk. Mat.-Fys. Medd.* **28**, No. 8 (1954).
- <sup>12</sup>R. B. Alexander, G. Dearnaley, D. V. Morgan, J. M. Poate, and D. Van Vliet, in *Proceedings of the European Conference on Ion Implantation*, Reading, 1970 (P. Peregrinus, Stevenage, Herts, England, 1970), p. 181.
- <sup>13</sup>G. Della Mea, A. V. Drigo, S. Lo Russo, P. Mazzoldi, and G. G. Bentini, *Rad. Effects* **13**, 115 (1972).
- <sup>14</sup>J. Lindhard and M. Scharff, *K. Dan. Vidensk. Selsk. Mat.-Fys. Medd.* **27**, No. 15 (1953).
- <sup>15</sup>S. T. Picraux, J. A. Davies, L. Eriksson, N. G. E. Johansson, and J. W. Mayer, *Phys. Rev.* **180**, 873 (1969).
- <sup>16</sup>K. Björkqvist, B. Cartling, and B. Domeij, *Rad. Effects* **12**, 267 (1972).
- <sup>17</sup>J. H. Barrett, *Phys. Rev. B* **3**, 1527 (1971).